



The possible benefits of *Garcinia kola* and curcumin on diabetes-induced aorta damage in the male rats with transected sciatic nerve: An experimental study

Gamze Altun ^{ID}1, Osman Furkan Gedik ^{ID}2, Merve Kurtulmuş ^{ID}2, Göksu Gökteş ^{ID}2, Yasemin Elif Eroğlu ^{ID}2, Hale Nur Özler ^{ID}2, Melih Tezel ^{ID}2, Hale Gemicici ^{ID}2, Süleyman Kaplan ^{ID}1,3

1 Department of Histology and Embryology, Faculty of Medicine, Ondokuz Mayıs University, Samsun, Türkiye

2 Faculty of Medicine, Ondokuz Mayıs University, Samsun, Türkiye

3 The Nelson Mandela African Institution of Science and Technology, Arusha, Tanzania

Received: 22.09.2025; Revised: 10.02.2026; Accepted: 16.02.2026

Abstract

Background: The aim of this study is to evaluate the degenerative effects of diabetes on the aorta and the potential therapeutic advantages of herbal agents halting the progression of diabetes, using morphoquantitative, light, and electron microscopy, and immunohistochemical methods. In diabetic rats with sciatic nerve transection, severe systemic inflammation can lead to significant changes in vascular morphology. Therefore, it was hypothesized that the combination of neuropathic pain and diabetes would create a more clinically significant pathophysiological picture.

Methods: The study groups consisted of 35 randomly selected Wistar albino rats: Healthy control group (Cont) (n=7), Sham that underwent the operation (n=7), Diabetes mellitus group induced by streptozotocin (DM) (n=7), diabetes treated with 200 mg/kg/day *Garcinia kola* (GK) (DM+GK) (n=7), and 300 mg/kg/day Curcumin (Cur) is administered to treat diabetes in the DM+Cur group (n=7). A neuropathic pain model was induced by performing a vein graft after sciatic nerve incision in all groups except the control group. 50 mg/kg (a single dose) of streptozotocin has been used for the induction of diabetes. Histopathological, ultrastructural, and immunostaining for anti-caspase-3 and anti-VEGF-A were evaluated.

Results: Degenerative changes were found in the diabetic aorta. Partial disruption of elastic fiber integrity in the tunica media was observed in the GK-treated group. Anti-caspase-3 positivity was intense in the DM rats. Anti-VEGF-A staining was low in the DM but higher in DM+Cur compared with DM+GK. The tunica media thickness decreased significantly in the DM and treatment groups compared to the Sham group.

Conclusion: Diabetes damages aortic elastic fibers. Cur can induce anti-VEGF-A expression, which is reduced in diabetes. Both curcumin and GK inhibit diabetes-induced apoptosis, with Cur exerting a more substantial protective effect on the aorta.

Keywords: Aorta, Apoptosis, Curcumin, Diabetes Mellitus, *Garcinia Kola*

DOI: 10.5798/dicletip.1906467

Correspondence / Yazışma Adresi: Gamze Altun, Department of Histology and Embryology, Faculty of Medicine, Ondokuz Mayıs University, 55139, Samsun, Türkiye, e-mail: gamzeyayla.omu@gmail.com

Kurkumin ve *Garcinia Kola*'nın diyabetik aort hasarı üzerindeki iyileştirici etkileri: Deneysel bir çalışma

Öz

Giriş: Bu çalışmanın amacı, diyabetin aort üzerindeki dejeneratif etkilerini ve terapötik bitkilerin diyabetin ilerlemesini durdurucu potansiyel terapötik avantajlarını, morfolojik, ışık ve elektron mikroskopisi ile immünohistokimyasal yöntemler kullanarak değerlendirmektir. Siyatik sinir kesisi modeli oluşturulan diyabetik sıçanlarda gelişen şiddetli sistemik inflamasyon, vasküler morfolojide önemli değişikliklere yol açabilir. Bu nedenle, nöropatik ağrı modeli ile diyabet hastalığının birlikte klinik açıdan daha anlamlı bir patofizyolojik tablo oluşturacağı düşünülmüştür.

Yöntemler: Çalışma grupları rastgele seçilmiş 35 Wistar albino sıçandan oluşmuştur: Sağlıklı kontrol grubu (Kont) (n=7), cerrahi kontrol grubu olan Sham grubu (n=7), streptozotosin ile indüklenen diyabet grubu (DM) (n=7), 200 mg/kg/gün *Garcinia kola* (GK) ile tedavi edilen diyabet grubu (DM+GK) (n=7) ve DM+Kur grubunda diyabeti tedavi etmek için 300 mg/kg/gün Kurkumin (Kur) uygulanan grup (n=7). Kontrol grubu hariç tüm gruplarda siyatik sinir insizyonundan sonra ven grefti uygulanarak nöropatik ağrı modeli oluşturulmuştur. Diyabet indüksiyonu için 50 mg/kg (tek doz) streptozotosin kullanılmıştır. Histopatolojik, ultrastrüktürel ve anti-kaspaz-3 ve anti-VEGF-A için immün boyama değerlendirilmiştir.

Bulgular: Diyabetik aortada dejeneratif değişiklikler saptandı. GK ile tedavi edilen grupta tunika media'da elastik lif bütünlüğünde kısmi bozulma gözlemlendi. Anti-kaspaz-3 pozitifliği DM sıçanlarında yoğundu. Anti-VEGF-A boyaması DM grubunda düşük, ancak DM+Kur grubunda DM+GK grubuna kıyasla daha yüksekti. Tunika media kalınlığı, Sham grubuna kıyasla DM ve tedavi gruplarında anlamlı derecede azaldı.

Sonuç: Diyabet, aortun elastik liflerine zarar verir. Kur, diyabette azalan anti-VEGF-A ekspresyonunu tetikleyebilir. Hem Kur hem de GK, diyabetin neden olduğu apoptozu inhibe eder; ancak Kur aort üzerinde daha belirgin bir koruyucu etki gösterir.

Anahtar kelimeler: Aort, Apoptoz, Kurkumin, Diabetes Mellitus, *Garcinia Kola*.

INTRODUCTION

Diabetes mellitus (DM) has long been considered a serious health problem with multifaceted effects¹. DM is a disease with high morbidity that causes various metabolic complications and a decrease in health and quality of life. Chronic hyperglycemia due to DM causes long-term damage and functional loss in many organs². Cardiovascular diseases (CVD) constitute a primary complication of type 2 DM. For individuals who have type 2 diabetes and hypertension, cardiovascular disease increases the risk of macrovascular complications. Thus, alterations in the cardiac and vascular architecture of hypertensive and diabetic individuals substantially influence hemodynamic stress³. Chronic hyperglycemia and insulin resistance have a crucial function in the development of vascular complications, which are closely related to macrovascular and microvascular diseases⁴.

Microvascular complications of DM result in nephropathy, retinopathy, and neuropathy.

Furthermore, chronic diabetes mellitus also manifests macrovascular complications^{1,5}. Some studies have reported the impact of diabetes on arterial diameter^{6,7}, demonstrating that the aortic root in people with DM is smaller than that of non-diabetics. In DM patients, vascular diseases, characterized by reduced endothelium-dependent vasodilation and increased vascular smooth muscle cell contraction, are the essential causes of morbidity and mortality⁹. Besides the metabolic and inflammatory systemic effects triggered by diabetes, the neuroinflammatory effects revealed by sciatic nerve injury, modeled in peripheral nerve neuropathy, can trigger degenerative processes in the aorta. Based on this, our study focused on a diabetic rat model with sciatic nerve transection.

Endothelial dysfunction is closely associated with diabetic angiopathy^{8,10}. In our study, we aimed to evaluate anti-VEGF-A immunohistochemical staining to observe

diabetes-induced endothelial dysfunction. VEGF-A has several functions, including promoting endothelial cell migration, increasing blood vessel permeability, and promoting proangiogenic function¹¹. It is an essential regulator of neoangiogenesis and vasculogenesis, mediating effects such as enhanced vascular permeability, cell proliferation, and prevention of apoptosis¹².

Curcumin, a natural phenolic compound, has antimicrobial, anti-inflammatory, and antioxidant activity^{13,14}. It has been shown that a curcumin analog protects the aorta of mice against oxidative stress in type 1 DM¹⁵. However, evidence is also presented that curcumin suppresses angiogenesis in the aorta of non-diabetic and diabetic rats. While angiogenesis is essential for maintaining healthy tissues, controlling abnormal angiogenesis is a therapeutic goal¹⁶. It has been declared that kolaviron, a substance derived from *Garcinia kola* seeds, causes hypoglycemic effects in individuals with diabetes¹⁷. However, no evidence has been provided for the angiogenic effect of *Garcinia kola* in aortic tissue. In this regard, our study aimed to immunohistochemically examine the expressions of anti-caspase-3 and anti-VEGF-A in relation to the possible anti-angiogenic and anti-apoptotic activity of curcumin. Additionally, another aim of the current study is to determine the protective efficacy of these herbal agents at the cellular level, while also examining the potential degenerative effects of diabetes on aortic morphology at both the light and electron microscopic levels.

METHOD

Experimental Animals and Group Design

All experimental methods involving live animals used in the current study were approved by the Ondokuz Mayıs University Local Animal Experiments Ethics Committee (Approval number: 2019/49, date: October 22, 2019).

Additionally, formal approval was obtained for the use of aortic cadaver tissues (Application number: 68489742-604.01.03-E.2607, dated January 31, 2020). Each animal experiment was conducted in compliance with national and institutional standards for the care and treatment of laboratory animals. The experimental protocol in this study was implemented according to the ARRIVE (Animal Research: Reporting of In Vivo Experiments) guideline, which was developed to increase transparency and reporting quality. The 3Rs principle (Replacement, Reduction, and Refinement) was considered for all experimental procedures.

Thirty-five male Wistar albino rats (250–300 g), aged 10–14 weeks, were divided into five groups at random: Healthy control group (Cont) (n=7), Sham group that performed the surgical operation (n=7), Diabetes Mellitus induced by streptozotocin (DM) (n=7), Diabetes mellitus + *Garcinia kola* treatment (DM+GK) (n=7), and Diabetes mellitus + Curcumin treatment (DM+Cur) (n=7). The Cont group, which acted as the baseline, underwent no surgical procedures. A 10-mm segment of the sciatic nerve was excised from the Sham group, located 2 cm distal to the sciatic notch, and the nerve terminals were anastomosed using a vein graft. In the DM, DM+GK, and DM+Cur groups, an intraperitoneal injection of streptozotocin (STZ) at 50 mg/kg was administered to induce diabetes. Diabetes was diagnosed seventy-two hours post-administration of STZ¹⁸.

The DM+Cur group of rats received 300 mg/kg of curcumin (Sigma-Aldrich, USA) daily via intragastric gavage in olive oil for a consistent 28-day period^{18,19}. Rats in the DM+GK group received 200 mg/kg/day of *Garcinia kola* extract by intragastric gavage for seven days^{18,20,21}. The animals were kept in a 12-hour dark, 12-hour light cycle, humidity levels of 50–60%, and a room temperature until the day of euthanasia. Access to tap water and feed was

permitted ad libitum. All rats were housed individually during the experiment and euthanized after 90 days.

Preparation of streptozotocin

Animals in the diabetes and post-diabetes treatment (curcumin and *Garcinia kola*) group were administered 50 mg/kg streptozotocin (Sigma Chemical Company, USA) in citrate buffer (pH: 4.5, 0.1 M) for 4 hours or overnight. It was injected intraperitoneally. Blood samples were taken from the animals seventy-two hours after STZ injection, and blood glucose levels were measured using a glucometer (Roche Diagnostics GmbH, Mannheim, Germany). Animals with fasting blood glucose levels above a certain limit (≥ 250 mg/dL) were considered diabetic. Blood glucose levels were evaluated in rats at 15-day intervals. Additionally, on the 3rd and 7th days post-STZ injection, blood glucose levels were assessed using the same methodology, validating the consistency of the DM model.

Surgical Procedures and Cardiac Perfusion

Before the sciatic nerve transection, rats were anesthetized with ketamine (50 mg/kg, Ketalar®, Eczacıbaşı, İstanbul, Türkiye) and xylazine (10 mg/kg, Rompun®, Bayer, İstanbul, Türkiye). After harvest, the external jugular vein (approximately 2.1 mm in diameter and 11.3 mm in length) was inverted, washed with saline, and tied off at both ends. A 1 cm section of the sciatic nerve was removed 2 cm distal to the sciatic notch, and the nerve was anastomosed to the vein graft (Ethicon EH 7438G, Norderstedt, Germany) using 10-0 nylon sutures to suture the epineural sheath proximally and distally. For three days after surgery, a topical antibacterial spray (Pederipra, Hipra, Girona, Spain) and intramuscular cefazolin sodium were administered at doses of 4 mg/kg, 2 mg/kg, and 1 mg/kg, respectively, to prevent infection. Wound healing was tracked every day. The rats

were weighed, and their blood glucose levels were recorded. They were then sedated under general anesthesia after the experiment. Intracardiac perfusion used 2% paraformaldehyde and 2% glutaraldehyde fixative. Aortic tissues were then removed and fixed for further examination.

Stereological Analysis

Using a point-counting approach with a test grid of 2500 μm^2 , stereological investigations were performed to determine the volume fractions of layers in comparison to the entire vessel wall. Using light microscopy pictures acquired at $\times 4$ magnification (Olympus BX43 microscope with a camera and CellSens Entry software, Olympus, USA), the planimetric approach was employed to determine the average diameter of the aortic lumen and the thickness of the tunica media. Images magnified $\times 20$ were used to estimate the volume fraction. Two separate researchers conducted the analyses in a blinded manner. While tunica media thickness was evaluated at four sites per segment, aortic lumen diameter was measured on both the horizontal and vertical axes and averaged.

Paraffin and Resin Blocks

After fixation, the aortic vessel of a randomly selected animal from each group was dissected under a stereomicroscope, washed with phosphate buffer, and then processed for electron microscopy. Additionally, aortic tissue samples from each group were embedded in paraffin blocks after processing. Sample sections 5 μm thick were used for histopathological evaluation and immunohistochemical analysis. The resin-embedded blocks were sectioned into toluidine blue-stained semi-thin (500 nm) sections using an ultramicrotome (Thermo Scientific Shandon, USA). Thin (70 nm) sections were obtained using an ultramicrotome. It was stained in the Imaging and Characterization Unit, located within the same center, using the Leica EM AC20

Brand automatic contrasting system (Leica Microsystems GmbH, Germany). Histopathological evaluation was performed on images using a light microscope (Olympus BX43, Center Valley, PA, USA) and the CellSens Entry software (Olympus, Center Valley, PA, USA). In the histopathological evaluation, the aortic layers were examined separately. The groups were evaluated with respect to the density of elastic lamellae and potential deformations in the vessel wall.

Immunohistochemical Analyses

Anti-VEGF-A (dilution: 1/100, ab1316, Abcam, USA) and anti-caspase-3 (dilution: 1/50, ab4051, Abcam, USA) antibodies were assessed immunohistochemically based on their staining intensity to further evaluate the cellular alterations induced by diabetes and anti-diabetic treatment agents in the aortic tissue. A mouse- and rabbit-specific HRP/AEC chromogen kit (Abcam, USA) was used for immunohistochemistry. The Mayer's hematoxylin was used as a counterstain. As part of the immunohistochemical analysis, negative control groups were created by incubating the final section of each slide overnight at +4°C in phosphate-buffered saline (PBS). No positive staining was detected in the negative control groups.

Statistical Analyses

Statistical analyses were conducted using GraphPad Prism version 8.0 (GraphPad Software, San Diego, CA, USA). For assessment, data normality was evaluated using the Shapiro-Wilk test. For normally distributed data, a one-way ANOVA was used, and Tukey's post hoc test was used to evaluate multiple comparisons. For data that was not uniformly distributed, the Kruskal-Wallis test and Dunn's post hoc test were implemented. The results are presented as the mean ± standard deviation (SD) in accordance with the data distribution.

Statistical significance was defined to include a p-value of 0.05 or less.

RESULTS

Stereological Results

The DM+GK group exhibited a decrease in the volume fraction of the tunica intima relative to the entire vessel wall when contrasted with the Control group ($p = 0.037$). The average tunica medium thickness was significantly higher in the Sham group compared with the Cont group ($p = 0.002$). Conversely, it was significantly lower in the DM group than in the Sham group ($p = 0.002$). Likewise, the tunica medium thickness was considerably lower in the DM+GK and DM+Cur groups than in the Sham group ($p = 0.0004$ and $p = 0.003$, respectively).

In terms of the volume fractions of tunica adventitia and tunica media to the total vessel wall volume, there is no significant difference among groups ($p > 0.05$). The average aortic lumen diameter was similar ($p > 0.05$) between groups (Figure 1). The groups' coefficient of error (≤ 0.05) and coefficient of variation (CV) (≤ 0.2) are summarized in Table I.

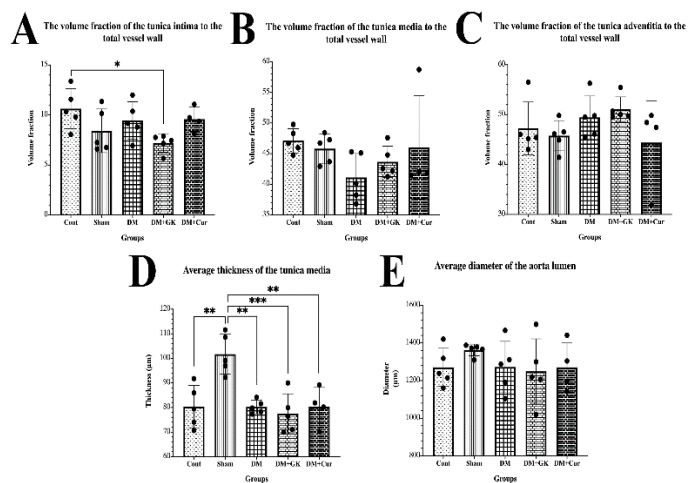


Figure 1. (A-E) Graphs presenting the statistical results of volume fractions and planimetric measurements for all groups are shown. Significant differences at the $p \leq 0.05$ level is indicated by “*”, while differences at the $p \leq 0.01$ and $p \leq 0.001$ levels are denoted by “**” and “***”, respectively.

Table I: The coefficient of variation (CV) and mean coefficient of error (CE) values

Groups	Cont	Sham	DM	DM+GK	DM+Cur
The tunica intima/total vessel wall (CV)	0.153	0.211	0.162	0.101	0.097
The tunica intima/total vessel wall (CE)	0.101	0.091	0.101	0.119	0.104
The tunica media/total vessel wall (CV)	0.037	0.042	0.078	0.048	0.143
The tunica media/total vessel wall (CE)	0.050	0.046	0.050	0.051	0.050
The tunica adventitia/total vessel wall (CV)	0.101	0.054	0.071	0.039	0.146
The tunica adventitia/total vessel wall (CE)	0.052	0.045	0.047	0.048	0.053
Average thickness of the tunica media (CV)	0.071	0.019	0.088	0.113	0.081
Average thickness of the tunica media (CE)	0.048	0.043	0.048	0.050	0.048
The mean diameter of the aortic lumen (CV)	0.066	0.065	0.028	0.085	0.068
The mean diameter of the aortic lumen (CE)	0.020	0.019	0.019	0.020	0.020

Histopathological Assessment of Aortic Tissue

Upon light microscopy, the vessels in the Cont group showed healthy morphology, with preserved structural integrity of the elastic fibers. Additionally, the endothelial cells exhibited a healthy structure, with clear nuclear boundaries (Figure 2a1-a3). Histological examination revealed that the tunica intima and media layers in the Sham and Cont groups had a normal appearance. The thickness of the tunica media layer was the same in both groups (Figure 2a1-b3). DM had a different histological structure than the Cont and Sham groups. The tunica media was thinner than in the Cont and Sham Groups (Figure 2c1-c3). The vaso vasorum in the tunica adventitia layer was healthy in the DM group, but the elastic fiber organization was poor (Figure 2c1). This group showed elastic fiber structural defects. The delineation of the endothelial cell borders inside the tunica intima layer was not distinctly identifiable (Figure 2c1-c3). The thickness of the tunica media in the DM+GK group was comparable to that in the Cont group. The endothelial cells exhibited a healthy morphology in the DM+GK group. It was observed that the structural integrity of the elastic fibers was not maintained in certain

areas (Figure 2d1-d3). The elastic fibers in the DM+Cur group had a healthy structure; however, the tunica media was thinner in this group compared with the Cont and Sham groups. Additionally, the boundaries of the nucleus and nucleolus of endothelial cells in the DM+Cur group were visible and had a healthy structure (Figure 2e1-e3).

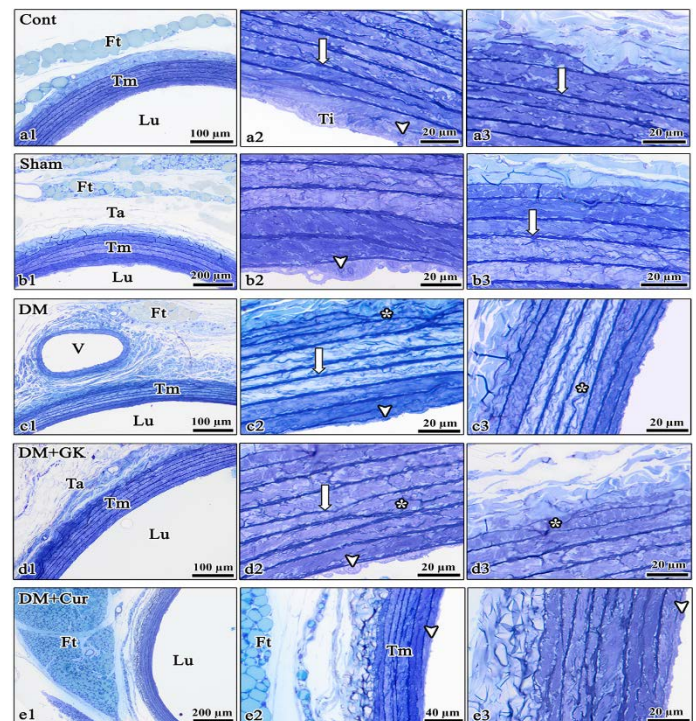


Figure 2. (a1-e3) Semi-thin sections from the Cont, Sham, DM, DM+GK, and DM+Cur groups are shown. **(a1-a3)** In the Cont group, the overall histological

structure of the aorta appears normal, with preserved structural integrity of the elastic fibers (arrow). The cytoplasm and nuclear boundaries of the endothelial cells (arrowhead) in the tunica intima are clearly distinguishable. **(b1-b3)** In the Sham group, the tunica media thickness is comparable to that of the Cont group, and the endothelial cells exhibit healthy morphology. No disruption in the organization of the elastic fibers is observed in this group. **(c1-c3)** In the DM group, the tunica media layer is thinner than in the Cont and Sham groups. The vaso vasorum (V) in the tunica adventitia appears healthy; however, **(c2, c3)** the structural integrity of the elastic fibers in the tunica media is partially disrupted (*) despite some areas remaining intact. The endothelial cells in the tunica intima are less distinct in this group (arrowhead). **(d1-d3)** In the DM+GK group, the tunica media thickness is normalized, although some disruption of elastic fiber organization (*) is still noted in certain regions, with some elastic fibers (arrow) retaining their integrity. **(e1-e3)** In the DM+Cur group, the elastic fiber layer is thinner compared to the Sham and Cont groups; however, the structural integrity of the elastic fibers (arrow) in the tunica media is well preserved. **(e2, e3)** The endothelial cells in the tunica intima also exhibit a healthy appearance (arrowhead). Cont, Control group; Sham, Sham group; DM, Diabetes mellitus group; DM+Cur, DM+Curcumin group; DM+GK, DM+*Garcinia kola* group; Ft: adipose tissue; Lu: lumen; Ta: tunica adventitia; Ti: tunica intima; Tm: tunica media. Resin section, Toluidine blue staining.

Ultrastructural Evaluation of Aortic Tissue

When the ultrastructural structures of all groups were examined electron microscopically, it was observed that the elastic fibers had a standard structure, and their structural integrity was preserved in the micrographs of the Cont group (Figure 3a1-a3). The presence of connections between the elastic layered structures is shown in the images. In the tunica media layer of the sham group, the structural integrity of the elastic fibers was preserved, allowing the internal elastic membrane to be distinguished (Figure 3b1-b3). The nuclear borders of endothelial cells in the Cont and Sham groups were evident (Figure 3a2 and b2). The borders of the endothelial cell nuclei of the DM group were observed to disappear. Deteriorations in the elastic fibers of this group were seen in detail (Figure 3c1-c2).

Additionally, the integrity of the internal elastic membrane structure was found to be lacking. The endothelial cells in the treatment groups exhibited normal morphology, with clear nuclear borders (Figure 3d1-e3). Nonetheless, the elastic fibers in the DM+GK group exhibited separation in certain areas. Vacuolization was noticeable in the endothelial layer of the DM+GK group (Figure 3d1-d3).

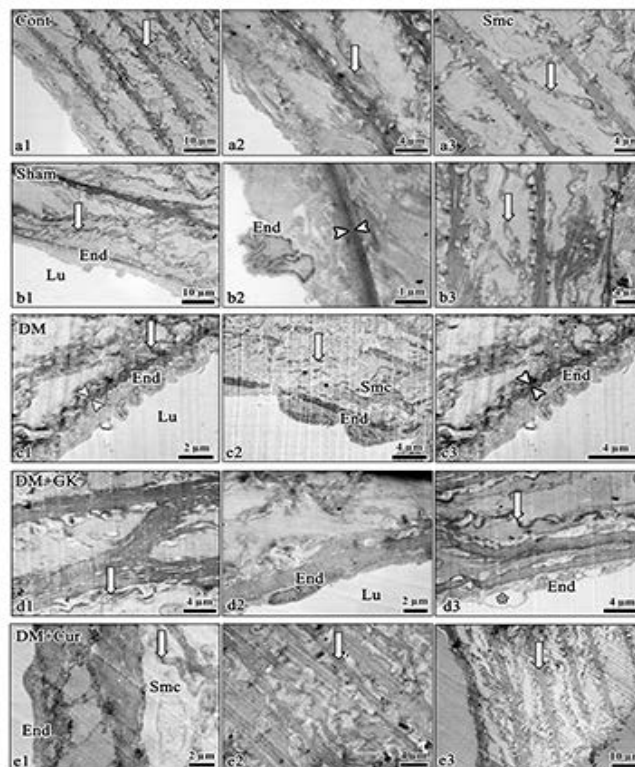


Figure 3. (a1-e3) Electron microscopic images of the Cont, Sham, DM, DM+GK, and DM+Cur groups are shown. **(a1-a3)** In the Cont group, elastic fibers exhibit a normal structure and maintain their integrity, with connections visible between elastic lamellae (arrow). **(b1-b3)** In the Sham group, the structural integrity of elastic fibers in the tunica media is preserved, and the internal elastic membrane (between arrowheads) appears normal. The endothelial cell (End) nuclear boundaries are intact, and elastic fibers between lamellae are clearly visible (arrow). **(c1-c3)** In the DM group, the nuclear borders of endothelial cells in the tunica intima are severely disrupted. The internal elastic membrane (between arrowheads) shows significant structural disruption, and the density of elastic fibers (arrow) in the tunica media is markedly decreased, with areas of fiber separation and poorly defined smooth muscle cell borders. **(d1-e3)** In the DM+GK and

DM+Cur groups, endothelial cells display normal morphology. **(d1-d3)** However, in the DM+GK group, separations in elastic fibers (arrow) are observed in some regions of the tunica media, along with vacuolization (*) in the endothelial layer. **(e1-e3)** In the DM+Cur group, the structural integrity of elastic fibers (arrow) in the tunica media is preserved. Cont, Control group; Sham, Sham group; DM, Diabetes mellitus group; DM+Cur, DM+Curcumin group; DM+GK, DM+*Garcinia kola* group; Lu, Lumen; Smc, Smooth muscle cell.

Immunohistochemical Analysis of Anti-Caspase 3 and Anti-VEGF-A in Aortic Tissue

Apoptotic activity in all groups was evaluated by anti-caspase-3 immunohistochemistry. No positive staining was shown in the aorta of the Cont group (Figure 4a1-a3). A positive staining was shown in the perivascular fat tissue of both the Sham and DM groups (Figure 4b1-c3). While low-intensity anti-caspase-3 positivity was shown in the tunica intima layer of the Sham group (Figure 4b1-b3), no staining was shown in the tunica intima layer of the Cont group (Figure 4a1-a3). Positive immunoreactions were shown in the tunica intima and some endothelial cells in the DM group (Figure 4c1-c3). Positive anti-caspase reactivity was also observed in the adipose tissue surrounding the vessel (Figure 4c1). However, no positive reaction was found in the tunica media of the DM group (Figure 4d1). While anti-caspase-3-positive staining was observed in endothelial cells of the treatment groups, positive reactions were also noted in the fatty tissue surrounding the vessels in the DM+GK group (Figure 4d1-d3). Additionally, anti-caspase-3-positive areas were observed in endothelial cells of the Cur-treated group (Figure 4e1-e3).

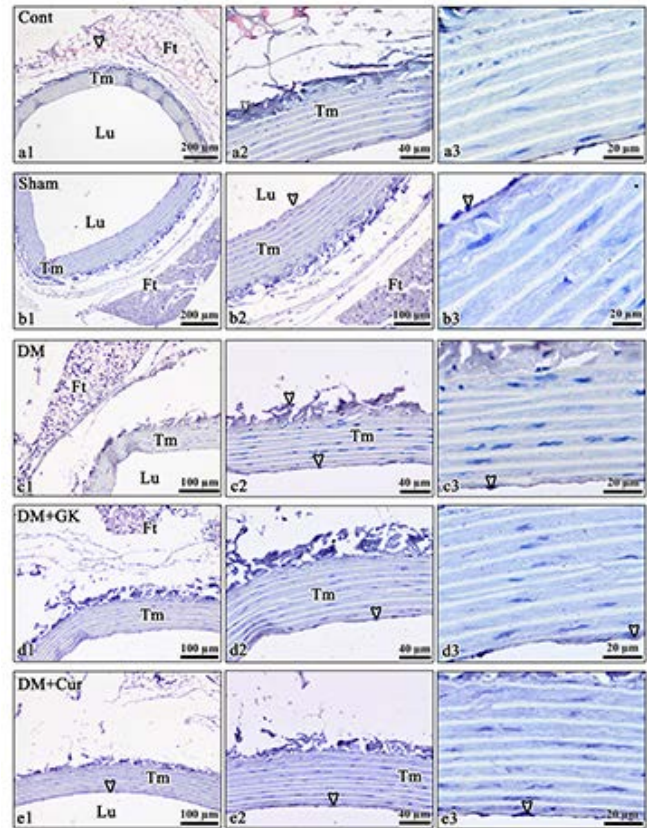


Figure 4. (a1-e3) Immunohistochemical staining with anti-caspase 3 in the Cont, Sham, DM, DM+GK, and DM+Cur groups is shown. **(a1-a3)** No positive staining was observed in the tunica media layer of the Cont group; however, positive staining (arrowhead) was detected in the adipose tissue surrounding the vessel. **(b1-b3)** In the Sham group, very weak anti-caspase 3 immunoreactivity (arrowhead) was observed in endothelial cells of the vascular tunica intima. **(c1-c3)** In the DM group, positive staining was observed in both endothelial cells (arrowhead) and adipose tissue within the tunica intima. **(d1-e3)** Similarly, anti-caspase-3-positive reactions (arrowhead) were observed in endothelial cells of the DM+GK and DM+Cur groups. **(d1-d3)** Notably, positive staining was also observed in the adipose tissue layer in the DM+GK group. **(c1-c3)** Unlike the other groups, the DM group exhibited strong positive staining in the tunica adventitia. Cont, Control group; Sham, Sham group; DM, Diabetes mellitus group; DM+Cur, DM+Curcumin group; DM+GK, DM+*Garcinia kola* group; Lu, Lumen; Smc, Smooth muscle cell; Ft, Adipose tissue; Tm, Tunica media. Mayer's hematoxylin was used for counterstaining.

Upon evaluating the anti-VEGF immunohistochemical stainings across the groups, pronounced staining was noted in every layer of the control group (Figure 5a1-a3). The tunica media layer of the Sham group exhibited low-intensity staining, while the tunica intima and adventitia layers exhibited intense staining (Figure 5b1-b3). Low-intensity anti-VEGF-A expression was found in the tunica media and intima of the DM group (Figure 5c1-c3). Positive staining was detected in some parts of the DM+GK and DM+Cur groups (Figure 5d1-e3). However, there was a low-intensity anti-VEGF-A expression in the tunica adventitia layer of the DM+GK group (Figure 5d1-d3). Intense anti-VEGF-A staining was observed in the DM+Cur. Especially, strong immunostaining in the vaso vasorum was observed in this group (Figure 5e1-e3).

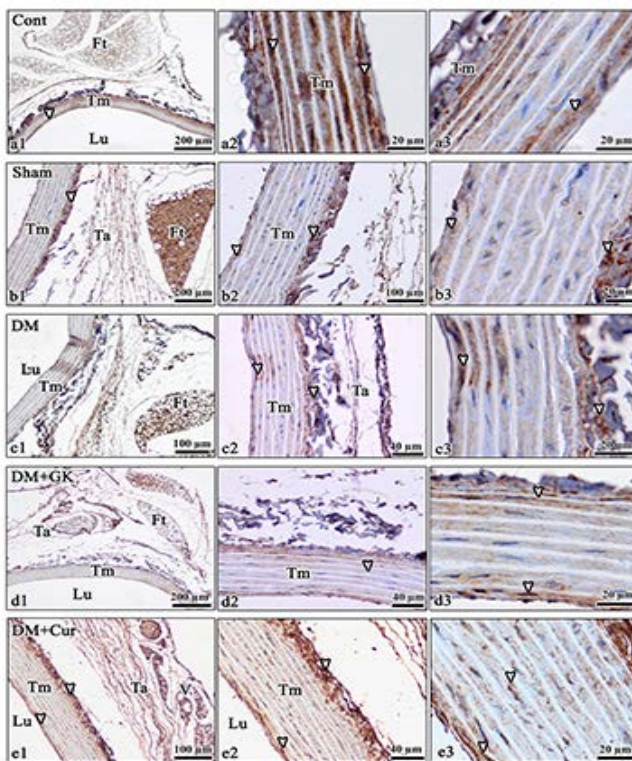


Figure 5. (a1-e3) Immunohistochemical staining for anti-VEGF-A in the Cont, Sham, DM, DM+GK, and DM+Cur groups. **(a1-a3)** The Cont group showed intense positive staining (arrowhead) in the tunica intima, media, and adventitia. **(b1-b3)** In the Sham group, intense staining was observed in the tunica

intima and adventitia, while staining in the tunica media was low. Intense staining was also noted in the adipose tissue. **(c1-c3)** The DM group exhibited weak anti-VEGF-A staining (arrowhead) in some areas of the tunica media, positive staining in some endothelial cells of the tunica intima, and intense staining in the tunica adventitia. **(d1-e3)** Both DM+GK and DM+Cur groups showed positive staining in parts of the tunica media. The DM+GK group displayed low intensity staining in the tunica adventitia, whereas the DM+Cur group showed intense staining in this layer. **(e1-e3)** Notably, strong staining was observed on the walls of the vaso vasorum (V) in the tunica adventitia of the DM+Cur group. Cont, Control group; Sham, Sham group; DM, Diabetes mellitus group; DM+Cur, DM+Curcumin group; DM+GK, DM+*Garcinia kola* group; Ft: adipose tissue; Lu: lumen; Ta: tunica adventitia; Tm: tunica media. Mayer's hematoxylin was used for counterstaining.

DISCUSSION

This study assessed the possible therapeutic roles of GK and Cur in reducing arterial damage and investigated how DM impacted the aortic wall. Our immunohistochemical and ultrastructural investigations revealed significant alterations in aortic tissue from diabetic rats. These changes included altered VEGF-A expression, increased apoptosis, and reduced elastic fiber integrity, all of which were partially restored by GK and Cur therapies. Using morphological, ultrastructural, and immunohistochemical techniques, the current study compares the therapeutic benefits of these agents on diabetes-induced aortic damage. On aortic structure and the molecular balance between neovascularization (via VEGF-A) and apoptosis (via caspase-3), even though the vascular protective role of Cur has been previously investigated. Furthermore, by simulating intricate clinical conditions, the use of a neuropathic pain model in diabetic rats enhances translational value. This early investigation demonstrates the potential of natural substances to alter key pathways underlying diabetic vascular problems.

Angiogenic activity in the adipose tissue in the Sham group was greater than DM group, as

indicated by anti-VEGF-A immunostaining. At the same time, VEGF-A expression was more elevated in the adipose tissue in the DM group. Given that adipocytes' amplification of VEGF-A stimulates angiogenesis²². This suggests the DM and Sham groups had active neovascularization. The increased expression of anti-VEGF-A in the adipose tissue and endothelium of the Sham group most likely indicates VEGF-mediated angiogenesis triggered by inflammatory processes²³. The increased VEGF-A expression observed in the DM group may reflect the balance between anti-inflammatory and pro-inflammatory cytokines following sciatic nerve transection. VEGF-A, a direct pro-angiogenic marker that plays a key role in angiogenesis, is released by various cytokines. However, more studies are needed regarding the effects of the peripheral neuropathy model on diabetic vascular damage²⁴.

By enhancing capillary permeability and promoting pathological angiogenesis, VEGF-A significantly contributes to endothelial dysfunction and microvascular complications in diabetes^{25,26}. Therefore, therapeutic modification of VEGF-A signaling has emerged as a target for managing diabetic vascular problems²⁷. Our findings, however, showed that Cur raised VEGF-A levels, especially in the vaso vasorum wall, rather than decreasing VEGF-A expression in diabetic aortas. With proangiogenic actions at low levels and antiangiogenic effects at higher concentrations, Cur's dual role in angiogenesis may be dose-dependent²⁸. VEGF-A-mediated neovascularization may have been accelerated by our high-dose Cur therapy, suggesting a convoluted and situation-specific process.

On the other hand, in line with its established ability to downregulate VEGF and its receptors, GK exhibited an inhibitory effect on VEGF-A production²⁹. There is insufficient information on GK's precise effects on angiogenesis, which necessitates further research, despite indicating

that GK may not be as effective as Cur in achieving neovascularization.

In accordance with earlier results showing increased caspase-3-mediated apoptosis in vascular tissues during diabetes, our immunohistochemical investigation revealed increased apoptotic activity in the diabetic aortas³⁰. In this regard, GK and Cur treatments showed their protective effects on vascular smooth muscle cells by successfully suppressing apoptosis in the tunica media. Maintaining vascular integrity and avoiding diabetic vascular problems depend heavily on this anti-apoptotic characteristic. These results were corroborated by ultrastructural analysis, which revealed that Cur preserved the elastic fiber architecture better than GK, most likely because of its superior aortic wall restorative properties. Similar protective effects of Cur on the remodeling of elastic lamellae in vascular tissues have been documented in earlier research³¹.

Given the low bioavailability of curcumin, the efficacy-safety balance and pharmacokinetic properties reported in the literature were taken into consideration when determining antioxidant doses and application durations. The low bioavailability of Cur necessitated a longer application period³², while a shorter application period was deemed sufficient for GK. Sciatic nerve injury and diabetes mellitus can cause not only local but also systemic inflammatory effects. Therefore, a 90-day follow-up period was preferred to evaluate the transition of inflammation from the acute to the chronic phase and its implications for distant organs such as the aorta. Furthermore, this period is suitable for the establishment of chronic diabetes mellitus and the manifestation of permanent tissue damage in experimental models. In the literature, follow-up periods of 75–90 days are commonly used in STZ-induced diabetes models³³. Indeed, Adaramoye and Adeyemi (2006) reported that kolavirone

showed antidiabetic effects within the first 3–7 days³⁴. In diabetes treatment, suppressing oxidative stress and inflammation in the early stages can help maintain long-term tissue integrity even after treatment is discontinued, a phenomenon explained by the concept of metabolic memory³⁵. In this context, future studies are needed to investigate the role of *Garcinia kola* at different doses and durations on the vascular system.

Stereological analysis showed that the tunica media was thinner in diabetic rats than in Sham rats. The thickness of the tunica media was not significantly altered by treatment with GK or Cur, indicating that their protective methods may involve functional and molecular modulation rather than gross morphological restoration.

Study Limitations

The lack of a diabetes-only group without neuropathic pain or sciatic nerve transection is a study constraint. This would have allowed for a more focused assessment of the effects of hyperglycemia and diabetes on VEGF-A expression and vascular morphology. This strategy was founded on strong earlier data showing vascular alterations brought on by diabetes.

CONCLUSION

The degenerative effects of diabetes on the aortic wall may occur when apoptosis is induced in the tunica intima and media. *Garcinia kola* and curcumin can inhibit apoptosis in vascular smooth muscle cells. Additionally, curcumin has healing effects on improving the elastic integrity of the aortic wall, which is impaired due to diabetes. The induction of anti-VEGF by curcumin in the endothelial layer may indicate neovascularization. On the other hand, in diabetic aorta, *Garcinia kola* and curcumin can be considered treatment options for regulating VEGF and caspase-3 expressions. However, new dose-dependent studies on the

effects of both therapeutic agents on VEGF are needed.

Ethical Approval: All experimental methods involving live animals used in the current study were approved by the Ondokuz Mayıs University Local Animal Experiments Ethics Committee (Approval number: 2019/49, date: October 22, 2019). Additionally, formal approval was obtained for the use of aortic cadaver tissues (Application number: 68489742-604.01.03-E.2607, dated January 31, 2020).

Conflict of Interest: The authors declared no conflicts of interest.

Financial Disclosure: The authors declared that this study has received no financial support.

REFERENCES

1. Glovaci D, Fan W, Wong ND. Epidemiology of diabetes mellitus and cardiovascular disease. *Curr Cardiol Rep* 2019; 21(4): 21.
2. American Diabetes A. Diagnosis and classification of diabetes mellitus. *Diabetes Care* 2009; 32 (Suppl 1): S62–7.
3. Strain WD, Paldanius PM. Diabetes, cardiovascular disease and the microcirculation. *Cardiovasc Diabetol* 2018; 17(1): 57.
4. Petrie JR, Guzik TJ, Touyz RM. Diabetes, hypertension, and cardiovascular disease: clinical insights and vascular mechanisms. *Can J Cardiol* 2018; 34 (5): 575–84.
5. Beckman JA, Creager MA, Libby P. Diabetes and atherosclerosis: epidemiology, pathophysiology, and management. *JAMA* 2002; 287(19): 2570–81.
6. Androulakis AE, Andrikopoulos GK, Kartalis AN, et al. Relation of coronary artery ectasia to diabetes mellitus. *Am J Cardiol* 2004; 93 (9): 1165–7.
7. Lederle FA, Johnson GR, Wilson SE, et al. The aneurysm detection and management study screening program - Validation cohort and final results. *Arch Intern Med* 2000; 160 (10): 1425–30.
8. Chen XF, Wang JA, Lin XF, et al. Diabetes mellitus: is it protective against aortic root dilatation? *Cardiology* 2009; 112 (2): 138–43.

9. Liu Y, Wei J, Ma KT, et al. Carvacrol protects against diabetes-induced hypercontractility in the aorta through activation of the PI3K/Akt pathway. *Biomed Pharmacother* 2020; 125: 109825.
10. Endemann DH, Schiffrin EL. Endothelial dysfunction. *J Am Soc Nephrol* 2004; 15 (8): 1983–92.
11. Shibuya M. Vascular endothelial growth factor (VEGF) and its receptor (VEGFR) signaling in angiogenesis: a crucial target for anti- and pro-angiogenic therapies. *Genes Cancer* 2011; 2 (12): 1097–105.
12. Senger DR. Vascular endothelial growth factor: much more than an angiogenesis factor. *Mol Biol Cell* 2010; 21(3): 377–9.
13. Aggarwal BB, Sundaram C, Malani N, Ichikawa H. Curcumin: The Indian solid gold. *Adv Exp Med Biol* 2007; 595: 1–75.
14. Wang ME, Chen YC, Chen IS, et al. Curcumin protects against thioacetamide-induced hepatic fibrosis by attenuating the inflammatory response and inducing apoptosis of damaged hepatocytes. *J Nutr Biochem* 2012; 23(10): 1352–66.
15. Liu Y, Wang Y, Miao X, et al. Inhibition of JNK by compound C66 prevents pathological changes of the aorta in STZ-induced diabetes. *J Cell Mol Med* 2014; 18(6): 1203–12.
16. Dehghan MH, Mirmiranpour H, Faghihi-Kashani S, et al. Inhibitory effect of curcumin on angiogenesis in a streptozotocin-induced diabetic rat model: An aortic ring assay. *J Tradit Complement Med* 2016; 6 (4): 437–41.
17. Adaramoye OA. Antidiabetic effect of kolaviron, a biflavonoid complex isolated from *Garcinia kola* seeds, in wistar rats. *Afr Health Sci* 2012; 12 (4): 498–506.
18. Hamour HM, Marangoz AH, Altun G, Kaplan S. Neuroprotective effects of *Garcinia kola* and curcumin on diabetic transected sciatic nerve. *Biomed Mater* 2025; 20 (3).
19. Lee HY, Kim SW, Lee GH, et al. Turmeric extract and its active compound, curcumin, protect against chronic CCl₄-induced liver damage by enhancing antioxidation. *BMC Complement Altern Med* 2016; 16 (1): 316.
20. Ajayi SA, Ofusori DA, Ojo GB, et al. The microstructural effects of aqueous extract of *Garcinia kola* (Linn) on the hippocampus and cerebellum of malnourished mice. *Asian Pac J Trop Biomed* 2011; 1 (4): 261–5.
21. Oyagbemi AA, Omobowale TO, Olopade JO, Farombi EO. Kolaviron and *Garcinia kola* attenuate doxorubicin-induced cardiotoxicity in Wistar rats. *J Complement Integr Med* 2017;15(1): /j/jcim.2018.15.issue-1/jcim-2016-0168/jcim-2016-0168.xml.
22. Park J, Kim M, Sun K, et al. VEGF-A-expressing adipose tissue shows rapid beiging and enhanced survival after transplantation and confers IL-4-independent metabolic improvements. *Diabetes* 2017; 66 (6): 1479–90.
23. Kiguchi N, Kobayashi Y, Kadowaki Y, et al. Vascular endothelial growth factor signaling in injured nerves underlies peripheral sensitization in neuropathic pain. *J Neurochem* 2014; 129 (1): 169–78.
24. Laddha AP, Kulkarni YA. VEGF and FGF-2: Promising targets for the treatment of respiratory disorders. *Respir Med* 2019;156: 33-46.
25. Asselbergs FW, de Boer RA, Diercks GF, et al. Vascular endothelial growth factor: the link between cardiovascular risk factors and microalbuminuria? *Int J Cardiol* 2004; 93 (2-3): 211–5.
26. Hovind P, Tarnow L, Oestergaard PB, Parving HH. Elevated vascular endothelial growth factor in type 1 diabetic patients with diabetic nephropathy. *Kidney Int Suppl* 2000; 75: S56–61.
27. Aiello LP, Wong JS. Role of vascular endothelial growth factor in diabetic vascular complications. *Kidney Int Suppl* 2000; 77: S113–9.
28. Wang TY, Chen JX. Effects of Curcumin on Vessel formation insight into the pro- and antiangiogenesis of curcumin. *Evid-Based Compl Alt* 2019; 1390795.
29. Muhammad A, Funmilola A, Aimola IA, et al. Kolaviron shows anti-proliferative effect and down regulation of vascular endothelial growth factor-C and toll like receptor-2 in infected blood lymphocytes. *J Infect Public Heal* 2017; 10 (5): 661–6.

30. Barber AJ, Gardner TW, Abcouwer SF. The significance of vascular and neural apoptosis to the pathology of diabetic retinopathy. *Invest Ophthalmol Vis Sci* 2011; 52 (2): 1156–63.
31. Li X, Fang Q, Tian X, et al. Curcumin attenuates the development of thoracic aortic aneurysm by inhibiting VEGF expression and inflammation. *Mol Med Rep.* 2017; 16 (4): 4455–62.
32. Lopresti AL. The problem of curcumin and its bioavailability: could its gastrointestinal influence contribute to its overall health-enhancing effects? *Adv Nutr* 2018; 9(1): 41-50.
33. Akbarzadeh A, Norouzian D, Mehrabi MR, et al. Induction of diabetes by streptozotocin in rats. *Indian J Clin Biochem* 2007; 22(2): 60-4.
34. Adaramoye OA, Adeyemi EO. Hypoglycaemic and hypolipidaemic effects of fractions from kolaviron, a biflavonoid complex from *Garcinia Kola* in streptozotocin-induced diabetes mellitus rats. *J Pharm Pharmacol* 2006; 58(1):121-8.
35. Testa R, Bonfigli AR, Prattichizzo F, et al. The "Metabolic Memory" theory and the early treatment of hyperglycemia in prevention of diabetic complications. *Nutrients* 2017;9(5):437.